Biomacromolecules2

DATASET · FEBRUARY 2013

READS
30

5 AUTHORS, INCLUDING:

Philippe Douzenel
Université de Bretagne Sud
9 PUBLICATIONS **102** CITATIONS
SEE PROFILE

Olivier Sire
Université de Bretagne Sud
106 PUBLICATIONS **1,039** CITATIONS
SEE PROFILE

Does Water Activity Rule *P. mirabilis* Periodic Swarming? II. Viscoelasticity and Water Balance during Swarming

Elodie Lahaye,[†] Thierry Aubry,[‡] Vincent Fleury,[§] and Olivier Sire*[,†]

Laboratoire des Polymères, Propriétés aux Interfaces et Composites, Université de Bretagne-Sud, Campus de Tohannic, BP573 56017 Vannes Cedex, France, Laboratoire de Rhéologie, Université de Bretagne Occidentale, 6 avenue Le Gorgeu-CS93837, 29238 Brest Cedex 3, France, and Groupe Matière Condensée et Matériaux, UMR CNRS 6626, Université de Rennes 1, Campus de Beaulieu, 35042 Rennes Cedex, France

Received January 30, 2007; Revised Manuscript Received February 23, 2007

Following the analysis of the biochemical and functional properties of the *P. mirabilis* extra cellular matrix performed in the first part of this study, the viscoelasticity of an actively growing colony was investigated in relation to water activity. The results demonstrate that the *P. mirabilis* colony exhibits a marked viscoelastic character likely due to both cell rafts and exoproduct H-bond networks. Besides, the water loss by evaporation during migration has been measured, whereas the experimental determination of the water diffusion coefficient in agar has allowed us to estimate the net water influx at the agar/colony interface. These data drive us to propose that a periodic increase of the water activity at the colony's periphery, mainly due to the drastic surface to volume ratio increase associated with swarming, causes the periodic and synchronous cessation of migration through the dissociation of exoproduct networks, which in turn strongly alters the matrix viscoelasticity.

Introduction

Bacterial biofilms and colonies exhibit complex dynamics that link, in space and time, the behavior of a large number of individual cells. This is well exemplified by colony patterns, which have been well documented.[1,2] Hence, because of cell-to-cell interactions, a population behavior emerges, which exhibits new features absent in the planktonic forms of bacterial life. Regarding such complex dynamics, the case of *Proteus mirabilis* is particularly interesting. In this system, one observes a robust synchronicity and periodicity that do not seem to rely on the production of chemical triggers[3] usually reported in the development of biofilms.[4,5] We thus hypothesize that global colony properties may be the cause of this unique behavior, namely, the periodic swarming based on the alternation of the swarmer and vegetative morphotypes. In the preceding article,[6] we analyzed the biochemical properties of the extracellular matrix (ECM) of a *P. mirabilis* colony; it was characterized as a binary mixture of exopolysaccharides (EPS), glycine betaine, a potent osmoprotectant, and an unexpected phenoglycolipid (PGL), which so far has only been observed in the *Mycobacterium* genus. Besides, the rheological properties of purified EPS were also investigated, and a marked viscoelastic behavior was observed. This behavior vanishes at subphysiologic concentrations (<300 g/L), which emphasizes the importance of water activity. It was proposed that *P. mirabilis* ECM behaves as a semicrystalline medium because polysaccharides and glycolipid compounds were observed to auto-organize and crystallize as spherulites. The next step must address the behavior of the whole intact colony to match the ECM and colony's rheological properties. As discussed in the preceding article, the concomitant presence of a small EPS compound (MW of 1 kDa) and glycine betaine associated to a relatively low ECM hydration together suggest that the resulting low water activity (a_w) may play a prominent role in the control of *P. mirabilis* periodic swarming. In fact, the factors that are responsible for periodic swarming cessation remain unknown. To get better insights on this phenomenon, the rheological properties of the colony are investigated in light of water transfer at the interfaces during a swarming phase. Particular attention is paid to the concomitant alteration of the geometry of the colony because swarming induces a large increase of the surface to volume ratio (SVR). The data presented here lead us to propose that the stop signal may derive from a marked alteration of the slime mechanical properties, which in turn is due to a significant increase in a_W.

Experimental Section

Strain, Media, and Culture Conditions. The *P. mirabilis* wild-type strain WT19 corresponds to the clinical isolate U6450[7] from a chronic urinary tract infection (UTI) involving renal stone formation. WT19 was grown in LB medium at 37 °C. To obtain homogeneous populations of swarmer bacteria, 200 μL of an overnight liquid culture was spread onto a LB agar (1.5%) plate, and incubated for 4 h at 37 °C. Population characterization is performed as described in the preceding article. For studying periodic swarming, a 3 μL inoculum was deposited at the center of a petri dish and was allowed to grow for up to 8 h on the same agar solid medium.

Experimental Techniques. *Scanning Electron Microscopy (SEM).* Vapor fixation of centrally inoculated *P. mirabilis* colonies was achieved according to Jones et al.[8] by collecting colonies during active migration and suspending them upside down over 10 mL of a 12.5% grade glutaraldehyde and 8% paraformaldehyde (Acros organics) aqueous solution in a sealed staining dish for 18 to 24 h at room temperature. After fixation, blocks of agar (1 cm^2) were cut off from the colony's edge and

* Corresponding author. E-mail : osire@univ-ubs.fr. Phone: ++ 33 297 017 148. Fax: ++ 33 297 017 071.
[†] Université de Bretagne-Sud.
[‡] Université de Bretagne Occidentale.
[§] Université de Rennes 1.

10.1021/bm070115w CCC: $37.00
Published on Web 03/14/2007

inoculum domains. Blocks were then progressively dehydrated in a series of ethanol solutions (70, 90, and 100%) before critical-point drying. The dehydrated blocks were then sputter coated with gold during 60 s and examined by using a JSM 6460LV (JEOL) scanning electron microscope.

Laser Scanning Confocal Microscopy. Transvere sections of colonies were performed by using a scalpel, and a print was deposited on a slide and visualized by fluorescence labeling using the *Bac*Light LIVE/DEAD bacterial viability staining kit (Molecular Probes). A 1:1 mixture of stain/stock solution (SYTO 9 and propidium iodide) was diluted 25-fold in pure water. Then, 150 μL of the dye solution was spread on the print of the colony, and a coverslip was deposited. Excitation was performed by using the Argon laser line at 458 nm. Live (green) SYTO 9 stained cells (475 nm long-pass filter for emission) and dead (red) propidium iodide-stained cells (570 nm long-pass filter for emission) were visualized with a Zeiss LSM510 confocal scanning laser device mounted on a Zeiss Axiovert200 M microscope (Carl Zeiss).

Rheology of the Colony. Viscoelastic properties of the whole intact colony were characterized with a controlled stress Carri-Med CSL 50 rheometer equipped with parallel plate geometry. Otherwise, experimental conditions were as described in the preceding article.

Tonometry. This technique is derived from the well-known air puff tonometry technique used to measure intraocular pressure.[9] It involves the application of a local strain, namely, an air puff to a surface, and the measurement of deformation. However, in the specific case presented here, a high-resolution scanning air puff tonometer was designed (SAPT). The principle of the SAPT is the following: a patch clamp micropipet (obtained with a pipet puller (Sega)), is used to blow the air puff onto the surface of the colony. This pipet may have a diameter as small as 10 μm. The data presented below were acquired with a 50 μm diameter pipet. In order to measure the deformation, a spot of light is shone on the surface. This spot of light is provided by a laser diode (12 mW, Melles Griot) and is guided all the way down to the end of the pipet by a glass fiber (HCP MO200T from SEDI) passing inside the pipet. This results in the formation of a spot at the exact location where the stress is applied. In response to the stress, the colony deforms more or less depending on its local compliance and relaxes once the stress has ceased. The time-resolved deformation (z alteration) is monitored by continuous video recording of the laser spot at the colony's surface. The intensity of the air puff is controlled manually and checked by using a manometer. This original technique, developed at the GMCM laboratory, is analogous to conventional creep tests but presents the major advantage of allowing us to probe various locations and hence investigate local rheological heterogeneities because the sample is itself mounted on a displacement stage (Newport). Accordingly, such a technique is used here to locally probe the viscoelastic properties of the intact colony with a submillimetric spatial resolution.

ATR-FTIR Spectroscopy. To determine the water diffusion coefficient in agar, diffusion experiments were performed by using ATR-FTIR spectroscopy.[10] The instrumentation is as described in the preceding article.[6] A thin agar layer ($e \approx 1.5$ mm) is deposited on a *ZnSe* crystal, and at $t = 0$, 3 mL of D_2O is delivered to the top of the agar. FTIR spectra are then continuously recorded for 40 min with a time step of about 2 min. Spectra are the mean of 128 scans with a 4 cm^{-1} spectral resolution.

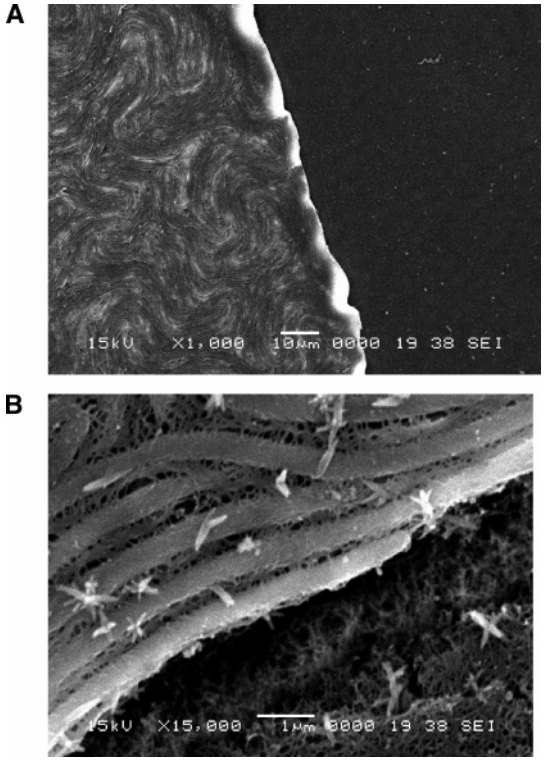

Figure 1. MEB snapshots of a swarming phase. Figure 1A displays bioconvection motions at the colony's edge (bar = 10 μm). A close-up is shown in Figure 1B, where entangled flagella are observed between adjacent swarmers (bar = 1 μm).

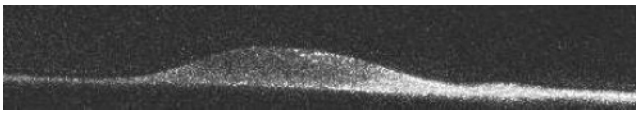

Figure 2. Confocal imaging of a terrace. A z section of a migrating colony is observed after dead/live fluorescent labeling. The central bell shape curve features the remnant of a consolidation phase (thickness of 45 μm). The thickness of the swarming phase is 16 μm. In the photograph, the swarmers migrate toward the right; the colony's edge is not shown.

Results and Discussion

Swarming Phase Dimensions. In order to investigate the swarming process, it was of primary interest to accurately characterize a typical migration phase in the 4D space. As outlined in the preceding article, active swarming lasts about 60 min and provides an increase in the radius of the colony by 2 mm. At the edge of the colony, the expansion process relies on active cell motility, which is best described by the so-called bioconvection motion, as shown in Figure 1A. Such fast (60 μm/s) bioconvection motions link individual swarmers into rafts (Figure 1B), whose cohesion is based on flagella entanglement as has already been observed.[8]

Thanks to LSCM, colony z sections were observed subsequent to fluorescent labeling and have allowed us to get information on the local thickness of the colony at a terrace and within a swarming phase. Figure 2 shows such a vertical section, which presents a thickness of 45 μm at the location of a terrace and 16 μm within the swarming phase.

It is thus possible to approximate the geometry of a particular migration phase at its final state as a hollow cylinder, that is, before the initiation of a new consolidation phase. If the inner and outer radii of this annulus are defined by r_{in} and r_{out} and h reflects the colony thickness, one can calculate the corresponding

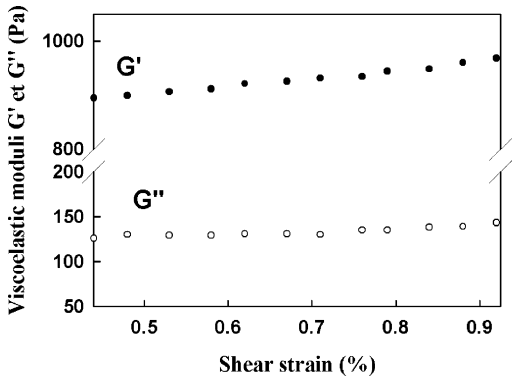

Figure 3. Viscoelastic behavior of an intact colony. Viscoelastic moduli G' and G'' as a function of shear strain.

surface and volume as follows.

$$S = \pi(r_{out}^2 - r_{in}^2) \text{ and } V = S \times h$$

Swarming results in a marked spreading of the bacterial population. Indeed, at the very beginning of a new active migration, the swarming population is packed at the terrace location, which, as seen from Figure 2, exhibits a bell curve pattern. Conversely, at the end of the migration, the population is spread on the agar surface as a thin (16 μm) film. This results in a drastic increase of the SVR. To illustrate and quantify this phenomenon, one may consider a colony exhibiting a radius of, for example, 3.2 cm; it yields a value for S and V of 3.89 cm^2 and 6.23 10^{-3} cm^3, respectively, which in turn yields a SVR $\approx$ 600 cm^{-1}. As biomass is kept constant during swarming, the recovered volume also features the initial population volume confined at the terrace location with a 300 μm width as deduced from LSCM observations. Hence, it derives that prior to swarming, the migrating population is packed on the top of the terrace (as a result of local cell divisions) and can be approximated by a rectangular section with a 300 μm base and a height value of $h = 220$ μm as calculated from $h = V/S$, V being equal to 6.23 10^{-3} cm^3. This approximation allows one to estimate a SVR of 45 cm^{-1} to be compared with the 600 cm^{-1} value at the completion of the swarming phase. Briefly, these calculations show that the SVR of the colony is locally increased by more than 10 times as a result of mass migration. The point will be discussed later because it is of importance for the water transfer at the interfaces.

Mechanical Properties of the Colony. To link the rheological experiments performed in the preceding article on purified EPS extracts to the multicellular entity behavior, the mechanical properties of an intact colony were investigated.

The experimental rheological investigation performed with the colony is of the same type as that used for EPS solutions, which was described in the preceding article. More precisely, simple oscillatory shear experiments were carried out in the linear viscoelastic regime in order to determine the elastic modulus G', characterizing the elastic energy stored in the colony, and the loss modulus G'', characterizing the energy dissipated by viscous friction within the colony. As shown in Figure 3, at a frequency of 1 Hz, the order of magnitude of the elastic modulus is about 1000 Pa at strain amplitudes lower than 1%, whereas the loss modulus is about 10-fold lower. This result clearly shows that the linear viscoelastic behavior of the colony is mainly and strongly elastic, meaning that its structure is much more cohesive than dissipative. In a complex fluid, such a behavior, dominated by elasticity, is characteristic of a 3D network structuring.[11] This structuring is probably due to the 3D organization of swarmers, entangled via flagella into stacked rafts, as discussed above.

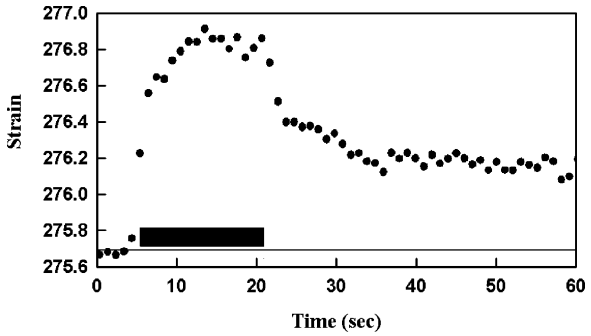

Figure 4. Tonometry and viscoelastic behavior. The Figure displays the response curve of the colony's periphery subsequent to an air puff. The horizontal black bar features the time interval during which the strain is applied.

Besides, in order to determine the colony's resistance to flow, creep measurements have been carried out, measuring Newtonian viscosity at very low shear rates ($\sim 10^{-4}$ s^{-1}). The results show that the zero shear Newtonian viscosity is about 50.000 Pa·s. Such a very high viscosity level shows that the colony very strongly resists shear flows, which makes good sense insofar as the structure is of the network type.

Following these experiments, we turned to tonometry in order to locally probe the mechanical properties of the colony. As mentioned in the Experimental Section, this experimental design allows one to monitor the viscoelastic properties in distinct spatial domains. Because swarmers and hence cell motility are restricted to the very edge of the colony, it was of interest to look for discontinuities in the mechanical properties of the colony in spatial domains that exhibit distinct motility status. To first validate the tonometry method for colony monitoring, a strain was applied at the periphery of the colony (Figure 4).

Figure 4 clearly shows that the colony quickly responds to the strain by a local deformation, which progressively reaches a plateau. When the strain is removed, this deformation partially vanishes as the system relaxes with a decreasing exponential pattern, even though it does not return to its initial value (featured by the gray baseline in Figure 4): at 60 s, that is, a delay twice the duration of the imposed stress, the colony has only relaxed at 50% of the maximal deformation. This pattern is typical of viscoelastic behavior and has been already observed by performing creep tests on various biofilms.[12]

Second, we probed the linearity between strain intensity and the colony's response in two distinct domains: the colony's edge (Figure 5A) and the last but one terrace (Figure 5B).

In Figure 5A, two pulses are sequentially performed on an actively migrating wave by doubling the intensity of the second air puff as compared to the first one. It is observed that the system responds quite linearly because the resulting deformations are roughly proportional to the triggering strain. In contrast, if the test is performed in a more inner domain exhibiting no motility (Figure 5B), the system response is not more linear because doubling the stress results in an unaltered deformation. From these findings, it is clear that the mechanical properties of the colony are not homogeneous throughout the colony but have heterogeneities associated with the motility status of the considered domain.

Semicrystallinity of the Colony. In the first part of this work, phase transitions and spherulite-like crystalline objects have been observed on purified ECM compounds such as EPS or PGL. One may question whether such crystals could be mere artifacts or whether they simply do not form in a growing colony.

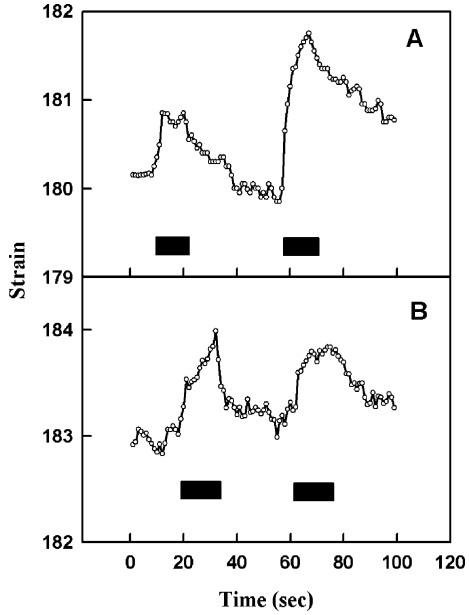

Figure 5. Viscoelastic heterogeneities within the colony. Two successive strains of increased intensities (×2) are applied at the last more recent (A) and last but one (B) terraces. Differences in the response linearity are shown.

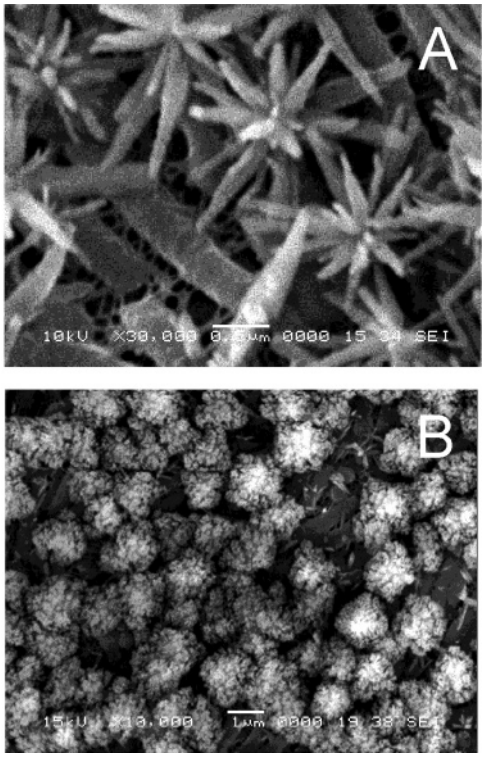

Figure 6. MEB snapshots of crystal objects observed in colonies. The Figure displays spiked crystals observed at the inoculum (A) and spherulite-like objects observed close to the periphery (B). A, bar = 0.5 μm; B, bar = 1 μm.

Accordingly, SEM snapshots of colonies have been collected to detect the presence of crystalline objects.

Observations were hence performed at the inoculum (Figure 6A) and close to the periphery (Figure 6B). At the inoculum, numerous spiked crystal objects are observed with spikes of about 1 μm in length. These objects are very similar to those observed in purified EPS solutions, which have been allowed to age (Figure 13B in the preceding article). If one focuses on the periphery (Figure 6B), the crystalline objects that dominate

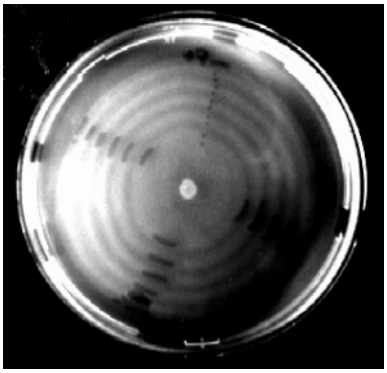

Figure 7. Colony pattern under water-vapor saturation conditions. A colony was grown at 37 °C in conditions of water-vapor saturation to investigate a possible limiting role of water loss during swarming. In these conditions, evaporation was reduced 2 times as compared to standard growing conditions.

are morphologically different because cotton flower-like spherical objects, exhibiting diameters of 1 μm are observed. Such patterns could be spherulites, similar to those observed in purified EPS and PGL extracts. The origin of such a dimorphism must be looked for in distinct exoproduct assemblies and cannot be due to variations in sample preparation because these two crystal morphologies, spiked and spherulite, are concomitantly observed within the same colony. As a whole, rheology and SEM observations allow one to assess the viscoelastic behavior of the colony and confirm that *P. mirabilis* exoproducts autoorganize in the presence of bacterial cells.

Water Balance during Swarming. Several clues drove us to hypothesize that water activity (a_W) may play a major role in *P. mirabilis* dynamics. The viscoelasticity of the colony is obviously a prerequisite for cell motility and hence for mass migration. The experiments performed on the ECM have demonstrated that these properties strongly depend on hydration status. However, swarming is periodic in nature; if one considers that a_W rules this periodicity, then it *de facto* implies that a_W must also vary periodically. Hydrodynamics of bacterial colonies is well documented.[13−16] Particular patterns have been ascribed to particular sets of advection diffusion models. However, little attention has been paid to the hydration status of a *P. mirabilis* colony. It is, therefore, necessary to estimate the water balance during a swarming phase. This balance reflects the water fluxes at the colony/atmosphere and agar/colony interfaces. To first estimate water availability, gravimetric measurements have been performed after 24 h of colonization at 37 °C, which results in a surface occupancy of 75% of the petri dish. This has allowed us to set that the 1.5% agar support and the colony present a hydration of 35 g_{water}/g_{agar} and 3.5 g_{water}/g_{colony}, respectively. Though not all of these water amounts are osmotically active because of a large pool of bound water interacting either with agar or ECM exoproducts,[17] the calculated relative water content likely reflects the osmotic conditions of the colony.

The total water loss due to evaporation, in the presence or in the absence of bacterial cells, represents 10% of the initial water amount (about 19 g/plate), which allows one to estimate the flux at the colony/atmosphere interface of $J = 1.38$ mg/cm^2/h. Because this flux is significant regarding the water content of the colony and may be critical for the swarming process, incubations have been performed at a saturating water vapor pressure (37 °C), which results in a 50% decrease of evaporation ($J = 0.73$ mg/cm^2/h). Figure 7 shows the resulting pattern of the colony, which remains unaltered compared to that in standard conditions (dry air).

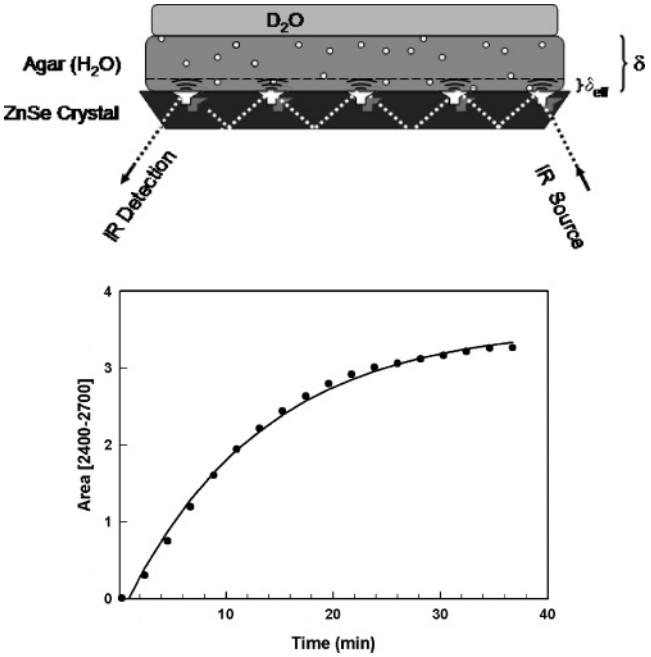

Figure 8. Measurement of the D_2O diffusion coefficient in agar at 37 °C. Figure 8A displays the experimental design used for the measurement of the D_2O diffusion coefficient in hydrated (H_2O) agar. The agar gel is deposited on a horizontal ZnSe ATR crystal. δ_{eff} and δ reflect the IR beam penetration depth and agar thickness, respectively. Figure 8B displays the time-dependent evolution of the infrared 2400−2700 cm^{-1} band area, which is characteristic of the ν_{O-D} stretching vibration. Data fitting allowed us to recover a relaxation time value τ of 15 min.

These global data allow one to calculate the flows at the swarming phase spatial scale. Keeping in mind the geometry of the problem and the time scale (1 h) described above, the water transfer during swarming can be estimated for an arbitrarily chosen colony radius of 3.2 cm. If one considers that the density of the colony is unity, then the migrating biomass is 6.23 mg including 4.84 mg of water. From the time integration of the surface expansion during the swarming phase (from $S_{t=0}$ = 0 cm^2 to $S_{t=60}$ = 3.89 cm^2), the evaporation is estimated at ~2.7 mg/h. This implies that partly because of the large increase of the SVR that characterizes the expansion of the colony, ~56% of the initial water content of the colony evaporates during migration. Because the edge of the colony does not dehydrate during swarming, this loss must, at least, be compensated by a water net influx at the agar/colony interface.

In order to estimate the water balance during a swarming phase, it is also necessary to estimate the agar → colony water influx. This flow depends on two parameters, that is, the water diffusion coefficient in agar and the water gradient at the agar/colony interface. If the latter may be deduced from the ratio of agar to colony hydrations (on average agar is 10 times more hydrated than the colony), the former requires estimating the water Einstein diffusion coefficient in agar in the physiological conditions of *P. mirabilis* in the growing phase. Purposely, this coefficient was derived from D_2O diffusion kinetic experiments performed in light water-hydrated agar. Hence, a light water−agar film was deposited on a horizontal ATR crystal thermostated at 37 °C, and the agar support was covered by a few milliliters of deuterated water. Because of isotopic replacement, the strongly absorbent ν_{O-D} vibration is shifted from 3400 cm^{-1} (ν_{O-H}) to 2450 cm^{-1}. This spectral shift allows us to detect the time evolution of $[D_2O]$ at the agar/*ZnSe* crystal interface (Figure 8A and B).

In the ATR mode, the depth of penetration of the IR beam into the sample is a function of the wavelength (λ), the refractive indexes of the crystal and the sample (n_2 and n_1, respectively), and the angle of incident radiation (θ). The depth of penetration δ_{eff} is given by the following formula.

$$\delta_{eff} = \frac{\lambda}{2\pi n_1 \sqrt{\sin^2\theta - \left(\frac{n_1}{n_2}\right)^2}}$$

Considering the ν_{O-D} frequency of ν = 2450 cm^{-1} (λ = 4.08 μm), which corresponds to the maximal absorption of D_2O, n_1 = 1.5 for the sample, n_2 = 2.4 for the *ZnSe* crystal, and θ = 45°, this yields a penetration depth value of δ_{eff} = 1.31 μm. The experimental D_2O kinetic diffusion curve exhibits an exponential pattern (Figure 8B) which is best fitted by the following equation

$$A(t) = a(1 - e^{-t/\tau})$$

where $A(t)$, a, and τ reflect the time evolution of the D_2O concentration estimated from the $A_{2400-2700}$ band area, the limit $[D_2O]_{t\to\infty}$, and the relaxation time, respectively. Data fitting allowed the recovery of a τ value of 15 min. The data treatment relies on the Fick−Einstein diffusion equation $\partial c/\partial t = D\ \partial^2 c/\partial x^2$, where c reflects the heavy water concentration (mol^{-1}) and D the diffusion coefficient.

During the time interval over which the D_2O diffusion front has not reached the $\delta - \delta_{eff} \approx \delta$ distance (featuring the agar gel thickness), the $[D_2O]$ at this coordinate remains null. If θ features this delay, it follows that

$$\text{in the time interval } 0 \le t \le \theta\ C_\delta = 0$$

$$\text{and thus } (gradC)_{0\to\theta} = \frac{0 - C_0}{\delta}$$

According to Fick's law, the mass of D_2O, m, diffusing through a unitary surface S = 1 per time unit at the δ coordinate and at time $t = \theta$ is as follows:

$$\left(\frac{dm}{dt}\right) = -DS\left(\frac{0 - C_0}{\delta}\right) = \frac{DSC_0}{\delta}$$

The water flux reaching the δ coordinate at time $t = \theta$ is proportional to the average water concentration in the δ_{eff} interval

$$\left(\frac{dm}{dt}\right)_\theta = \frac{DC_0}{\delta_0} = \frac{1}{2}\,\delta_{eff} C_\delta(\theta)$$

and consequently

$$C_\delta(\theta) = \frac{2D}{\delta\delta_{eff}}\,C_0$$

so that $(gradC)_{0\to\theta}$ when $t = \theta$ is

$$\left(\frac{\partial C}{\partial x}\right)_\theta = \frac{2\,\frac{D}{\delta\delta_{eff}}\,C_0 - C_0}{\delta}$$

and for $t > \theta$, C_δ increases as follows:

$$C_\delta(t) = \frac{2D}{\delta\delta_{eff}}\,C_0 + C_\delta(t - \theta)$$

The gradient at δ for $t > \theta$ becomes

$$\left(\frac{\partial C}{\partial x}\right)_{t>\theta} = \frac{2\frac{D}{\delta\delta_{eff}}C_0 + C_\delta(t-\theta) - C_0}{\delta}$$

By operating a time offset $t = t - \theta$, Fick's diffusion law at δ becomes

$$\frac{dm}{dt} = -D\frac{2\frac{D}{\delta\delta_{eff}}C_0 - C_0 + C_\delta(t)}{\delta}$$

In the ATR mode, only the D_2O mass encompassed in the δ_{eff} domain contributes to absorption, and one can check that

$$m(t) = \int dm = \int_0^t -\frac{D}{\delta}\left(2\frac{D}{\delta\delta_{eff}}C_0 - C_0 + C_\delta(t)\right)dt$$

Experimentally one measures the following.

$$m(t) = A(1 - e^{-t/\tau})$$

Because the water amount is equal to the $C_\delta \times V$ product, with $V = S \times \delta_{eff}$ (with $S = 1$) and C_δ equals the following

$$C_\delta = \frac{2D}{\delta\delta_{eff}}C_0 + C_\delta(t)$$

it follows that

$$m(t) = \left[\frac{2D}{\delta\delta_{eff}}C_0 + C_\delta(t)\right]\delta_{eff},$$

$$\text{which yields } \frac{2D}{\delta\delta_{eff}}C_0 + C_\delta(t) = \frac{A}{\delta_{eff}}(1 - e^{-t/\tau})$$

and

$$C_{\delta(t)} = \left(\frac{A}{\delta_{eff}} - \frac{2D}{\delta\delta_{eff}}C_0\right) - \frac{A}{\delta_{eff}}e^{-t/\tau}$$

Hence, Fick's diffusion law can be reformulated as follows:

$$\frac{dm}{dt} = \frac{A}{\tau}e^{-t/\tau} = \frac{D}{\delta}\left[C_0\left(1 - 2\frac{D}{\delta\delta_{eff}}\right) - \frac{A}{\delta_{eff}} + 2\frac{D}{\delta\delta_{eff}}C_0\right] + \frac{DA}{\delta\delta_{eff}}e^{-t/\tau}$$

This equation implies that

$$(1)\ \frac{D}{\delta}\left[C_0\left(1 - 2\frac{D}{\delta\delta_{eff}}\right) - \frac{A}{\delta_{eff}} + 2\frac{D}{\delta\delta_{eff}}C_0\right] = 0 \Rightarrow A = C_0\delta_{eff}$$

and

$$(2)\ \frac{A}{\tau} = \frac{DA}{\delta\delta_{eff}} \Rightarrow D = \frac{\delta\delta_{eff}}{\tau}$$

The water diffusion coefficient in agar at 37 °C may hence be calculated as follows:

$$D = \frac{\delta^*\delta_{eff}}{\tau} = 2.18\ 10^{-8}\ \text{cm}^2\ \text{s}^{-1}$$

This diffusion coefficient allows one to estimate the time evolution of the water gradient at the agar/colony interface. If one considers z as the vertical axis with the origin at the interface and the agar/colony relative hydration levels (10/1), the time evolution of the gradient follows the law

$$\frac{\partial C(z,t)}{\partial t} = D\frac{\partial^2 C(z,t)}{\partial z^2}, \text{ the solution of which is } C(z,t) = 4.5\,erf\left(\frac{z}{\sqrt{2Dt}}\right) + 5.5$$

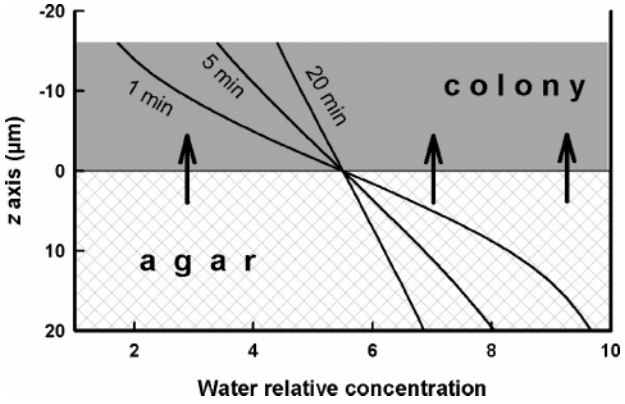

Figure 9. Simulation of water transfer at the agar/colony interface. The measurement of the D_2O diffusion coefficient in agar has allowed the simulation of the time evolution of the water concentration gradient at the agar/colony interface. The curves indicate the advance of the concentration front as a function of time at 1, 5, and 20 min. Water concentrations are relative with initial ($t = 0$) values of 1 and 10 in the colony and agar, respectively. Arrows indicate the direction of the net water flux.

Keeping in mind the thickness of the colony, that is, 16 μm, a simulation of the time evolution of the water concentration gradient at the agar/colony interface can be performed (Figure 9).

From this simulation, it is clear that the large SVR increase associated with colony expansion results in a progressive dilution of the colony as the swarmers migrate. Indeed, as shown in Figure 9, a 10 min delay is sufficient for the water content of the colony to be increased 4 times relative to its initial value.

The estimation of water balance during a swarming phase demonstrates that evaporation is not critical for the hydration of the colony. The measurement of the water diffusion coefficient in agar clearly indicates that the large increase (45 cm^{-1} up to 600 cm^{-1}) of the SVR promotes a significant net water influx from the agar to the colony, which, despite evaporation, must induce a significant increase in a_W within the colony. This dilution is minimally estimated 4 times, which must be analyzed in light of the EPS rheology experiments reported in the preceding article: a 3-fold dilution, from 300 to 100 g/L, results in a drastic decrease in EPS viscosity, which becomes close to that of water. However, a water net influx toward the colony occurs in a permanent regime. What differs between the consolidation and migration phases is that during consolidation, both biomass and water uptake increase, which prevents an increase of a_W; conversely, during the swarming process, the biomass is kept constant (no biosynthesis, no cell divisions), whereas water uptake is drastically increased because of the 10-fold increase of the SVR. From this, it necessarily follows a progressive dilution of the continuum in which the bacterial cells migrate. This dilution, that is, increase in a_W, must be of consequence to the exoproduct auto-assemblies as deduced from EPS rheology experiments (preceding article). The viscoelastic properties of these exoproducts and, consequently, of the whole

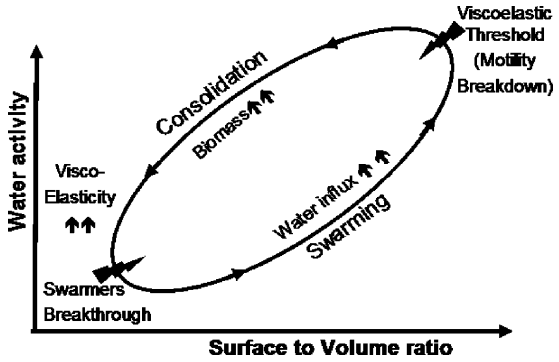

Figure 10. *P. mirabilis* limit cycle. The scheme describes the orbit along which the *P. mirabilis* cell population periodically travels. If one starts from the completion of a consolidation phase (lower left part of the cycle), the differentiated swarmer population starts mass migration, which progressively results in an increased SVR as the swarmers spread on agar and induced increased water uptake from agar. The increased a_W implies that the exoproduct concentration decreases below a subcritical value, which results in the dissociation of the ECM H-bond networks, which are essential for cell motility. Then, as a result of dedifferentiation toward the vegetative phenotype and extensive cell divisions (consolidation phase), the biomass locally increases, and the ECM viscoelastic properties are restored. This triggers a new swarming phase.

colony are critical for mass migration. Thus, a sharp transition of these properties toward more fluid conditions will impair the swarming process. Following the example of the first differentiation of a swimmer population deposited on a solid agar support that differentiates because of flagellum rotation hindrance,[18] it is postulated that a return to fluid conditions will drive dedifferentiation. This is well supported by the observation that an active swarmer dedifferentiates within minutes if placed in a liquid medium.[18] Moreover, it is expected that the more distant and, consequently, the longer the migration time, the more hydrated the swarmers. This 2D gradient is further increased by the fact that distal cellular rafts are in contact with agar domains, which have not yet been depleted in water except for evaporation. This makes sense because migration cessation and further dedifferentiation occurs at the very edge of the colony.

In a previous article,[19] we claimed that the dynamics on which the *P. mirabilis* symmetrical pattern relies must originate in a high-order information processing or in a global regulatory network. This implies that some signal is emitted, received, and integrated by the cell population. The present data focused on the concomitant approach of the mechanical properties of the colony, and exoproduct self-organization drives us to propose a simpler mechanism to warrant both the colony's radial symmetry and periodicity. In this framework, the periodic *P. mirabilis* migration/consolidation alternation results from a periodic a_W change in relation to considerable periodic SVR modifications between these two phases. These a_W changes are in turn of consequence for the exoproduct auto-organization, which strongly depends on the hydration status. Hence, *P. mirabilis* can be described as a biological oscillator, orbiting along a limit cycle, whose control parameters are physical (temperature and viscosity), chemical (a_W), and biological (biosynthesis and cell divisions) in nature (Figure 10). Simultaneously coping with expansion and cohesion requires that the multicellular entity must be able to stop repeatedly and in a concerted manner the expansion process achieved by the swarmer subpopulation. This is achieved by tuning exoproduct structures and expression levels so that the resulting continuum looses its intrinsic viscoelastic properties beyond a particular hydration level. Once this threshold is reached (Figure 10), the ECM continuum mechanical properties are no longer compatible with bacterial raft motility, which requires marked viscoelasticity. Hence, the duration of a swarming phase, the progressive ECM dilution, and the vanishing of the exoproduct molecular networks are the main parameters that determine both the periodicity and synchrony within a *P. mirabilis* colony.

Though the viscous properties of biofilms are yet to be investigated *in vivo*[12,20] and *in vitro*,[21] they were studied in physiological conditions in which the a_W was likely to be kept constant. Our results are coherent with the theoretical approach of the reaction−diffusion models, which show the interdependency of colony patterns and agar concentration.[22] Indeed, changing the agar concentration alters the amount of osmotically active water and hence the water availability for the colony. The present study also explains why *P. mirabilis*, along with many other strains, is able to swarm in a limited agar concentration range.[23,24] In conclusion, by its instability, that is, its sensitivity to hydration, the extracellular matrix prompts the cessation of mass migration, which puts it at the very center of the colony's dynamics.

More generally, one may question the relative roles of global properties and local chemical triggers on the control of the swarming process. As reported earlier, such chemical signals have only been detected in the very early phase of *P. mirabilis* colony formation.[25] To be active, such molecules must be able to diffuse efficiently on a large scale to achieve robust population synchronicity. This point may be critical in *P. mirabilis* colonies. The diffusivity of solutes in biofilms is one of the tracks to warrant the enhanced resistance of biofilms to antibiotics.[26−29] We have shown in the preceding article[6] that on average, the bacterial cells feature up to 80% of the colony's volume. With such a ratio, it has been shown that the relative effective diffuse permeability of various solutes was reduced to 20% of its value in the absence of bacterial cells.[27] Taking into account this reduced permeability, the large spatial domains to be correlated and the low a_W in *P. mirabilis* colonies, it follows that a signaling system based on diffusivity would likely be inefficient in properly pacing the expansion of the multicellular entity.

A last point that must be addressed is the relevance of such global regulation to the clinical impact. We demonstrate that *P. mirabilis* cells experience hyperosmotic conditions and propose that the low a_W within the colony is the main control parameter of the colony's dynamics. Such conditions are not far from those that prevail in human urine because humans can concentrate up to 4-times their urine as compared to blood osmolality, that is, up to 1200 mOsm/L. Moreover, this osmolality is known to vary significantly on a day−time scale even in healthy subjects. Interestingly, GB is significantly present in urine.[30] It is known that GB counteracts the deleterious effects of urea, the concentration of which is about 25 g/L, on epithelial cells. In the case of ascendant UTI, it has been inferred that osmoregulatory betaine uptake may promote growth in urine and the colonization of the human urinary tract by *E. coli*.[31] From this, it can be derived that the *P. mirabilis* osmotolerance evidenced *in vitro* is closely related to its ability to colonize the human urinary tract. Similarly, the relationship between swarming periodicity and UTI is also questionable because it has been reported that elongated swarmer cells were rarely observed in ascending UTI.[32] Swarming is a periodic process *in vitro*, which allows the colony to expand without the physical disruption of the multicellular entity. Conversely, one may consider that during UTI, transient, not necessarily periodic, swarming phases occur. As a result, as on agar plates, this

subpopulation, featuring only a minute part of the whole colony, achieves colony expansion on demand, with this demand resulting in a complex manner from changes occurring both within the colony (as a result of growth by example) and the environment. This point is apparently paradoxical, still virulence has been associated with swarming. If swimmers, as observed in liquid cultures, express no virulence factors, then dedifferentiated vegetative cells do, although at a lower level than the swarmers (Figure 3 in ref 33[33]). One of our previous studies[34] has clearly shown that vegetative cells exhibit a distinct IR spectral signature, that is, a distinct phenotype, from that of swimmers. Hence, one may question whether the low virulence of vegetative cells, compared to that of swarmers, is not sufficient to maintain a significant global virulence. Though many questions remain unanswered, the potential, at the population level, of a *P. mirabilis* colony and/or biofilm to grow and swarm in various physicochemical environments is well evidenced both *in vitro* and in the relatively versatile environment that prevails in the urinary tract.

Abbreviations

a_W: water activity
ECM: extra cellular matrix
EPS: exopolysaccharides
ATR-FTIR: attenuated total reflexion-Fourier transform infrared
GB: glycinebetaine
LB: Luria Bertani
LSCM: laser scanning confocal microscopy
PGL: phenoglycolipid
SAPT: scanning air puff tonometer
SVR: surface to volume ratio
UTI: urinary tract infection

Acknowledgment. We thank Professor B. Alpert for fruitful discussions and his contribution to the calculation of the water diffusion coefficient. We are also indebted to H. Guezenoc for his technical assistance in MEB experiments.

References and Notes

(1) Shapiro, J. A. Multicellularity: the Rule, Not the Exception. In *Bacteria as Multicellular Organisms*; Shapiro, J. A., and Dworkin, M., Eds.; Oxford University Press, New York, 1997; pp 14−49.
(2) Shapiro, J. A. The significances of bacterial colony patterns. *BioEssays* **1995**, *17*, 597−607.
(3) Matsuyama, T.; Takagi, Y.; Nakagawa, Y.; Itoh, H.; Wakita, J.; Matsushita, M. Dynamic aspects of the structured cell population in a swarming colony of *Proteus mirabilis*. *J. Bacteriol*. **2000**, *182*, 385−393.
(4) Eberl, L.; Christiansen, G.; Molin, S.; Givskov, M. Differentiation of *Serratia liquefaciens* into swarm cells is controlled by the expression of the flhD master operon. *J. Bacteriol.* **1996**, *178*, 554−559.
(5) Bassler, B. L.; Wright, M.; Silverman, M. R. Multiple signalling systems controlling expression of luminescence in *Vibrio harveyi*: sequence and function of genes encoding a second sensory pathway. *Mol. Microbiol.* **1994**, *13*, 273−286.
(6) Lahaye, E.; Aubry, T.; Kervarec, N.; Douzenel, P.; Sire, O. Does water rule *P. mirabilis* periodic swarming? I. Biochemical and functional properties of the extra cellular matrix. *Biomacromolecules* **2007**, *8*, 1218−1227.
(7) Koronakis, V.; Cross, M.; Senior, B.; Koronakis, E.; Hughes, C. The secreted hemolysins of *Proteus mirabilis*, *Proteus vulgaris*, and *Morganella morganii* are genetically related to each other and to the alpha-hemolysin of *Escherichia coli*. *J. Bacteriol*. **1987**, *169*, 1509−1515.
(8) Jones, B. V.; Young, R.; Mahenthiralingam, E.; Stickler, D. J. Ultrastructure of *Proteus mirabilis* swarmer cell rafts and role of swarming in catheter associated urinary tract infection. *Infect. Immun.* **2004**, *72*, 3941−3950.
(9) Levy, J.; Tovbin, D.; Lifshitz, T.; Zlotnik, M.; Tessler, Z. Intraocular pressure during haemodialysis: a review. *Eye* **2005**, *19*, 1249−1256.
(10) Thouvenin, M.; Linossier, I.; Sire, O.; Peron, J.-J.; Vallee-Rehel, K. Structural and dynamic approach of early hydration steps in erodable polymers by ATR-FTIR and fluorescence spectroscopies. *Macromolecules* **2002**, *35*, 489−498.
(11) Larson, R. G. *The Structure and Rheology of Complex Fluids*; Oxford University Press, New York, 1999.
(12) Shaw, T.; Winston, M.; Rupp, C. J.; Klapper, I.; Stoodley, P. Commonality of elastic relaxation times in biofilms. *Phys. Rev. Lett.* **2004**, *93*, 1−4.
(13) Matsushita, M.; Wakita, J.; Itoh, H.; Rafols, I.; Matsuyama, T.; Sakaguchi, H.; Mimura, M. Interface growth and pattern formation in bacterial colonies. *Physica A* **1998**, *249*, 517−524.
(14) Golding, I.; Kozlovsky, Y.; Cohen, I.; Ben-Jacobs, E. Studies of bacterial branching growth using reaction-diffusion models for colonial development. *Physica A* **1998**, *260*, 510−554.
(15) Lega, J.; Mendelson, N. A control-parameter dependent Swift-Hohenberg equation as a model for bioconvection patterns. *Phys. Rev. E: Stat. Phys., Plasma, Fluids, Relat. Interdiscip. Top.* **1999**, *59*, 6267−6274.
(16) Lega, J.; Passot, T. Hydrodynamics of bacterial colonies: a model. *Phys. Rev. E: Stat. Phys., Plasma, Fluids, Relat. Interdiscip. Top.* **2003**, *67*, 1−18.
(17) Mentré, P. In *L'eau dans la cellule. Une interface hétérogène et dynamique des macromolecules*; Masson ed., Paris, France, 1995.
(18) Alavi, M.; Belas, R. Surface sensing, swarmer cell differentiation and biofilm development. *Methods Enzymol*. **2001**, *336*, 29−40.
(19) Gué, M.; Dupont, V.; Dufour, A.; Sire, O. Bacterial swarming: a biochemical time-resolved FTIR-ATR study of *Proteus mirabilis* swarm-cell differentiation. *Biochemistry* **2001**, *40*, 11938−11945.
(20) Klapper, I.; Rupp, C. J.; Cargo, R.; Purvedorj, B.; Stoodley, P. Viscoelastic fluid description of bacterial biofilm material properties. *Biotechnol. Bioeng*. **2002**, *80*, 289−296.
(21) Tuinier, R.; Oomen, C. J.; Zoon, P.; Cohen Stuart, M. A.; de Kruif, C. G. Viscoleactic properties of an exocellular polysaccharide produced by a *Lactococcus lactis*. *Biomacromolecules* **2000**, *1*, 219−223.
(22) Mendelson, N. H.; Salhi, B. Patterns of reporter gene expression in the phase diagram of *Bacillus subtilis* colony forms. *J. Bacteriol*. **1996**, *178*, 1980−1989.
(23) Harshey, R. M. Bacterial motility on a surface: many ways to a common goal. *Annu. Rev. Microbiol.* **2003**, *57*, 249−273.
(24) Allison, C.; Hughes, C. Bacterial swarming: an example of prokaryotic differentiation and multicellular behaviour. *Sci. Prog*. **1991**, *75*, 403−422.
(25) Schneider, R.; Lockatell, C. V.; Johnson, D.; Belas, R. Detection and mutation of luxS-encoded autoinducer in *Proteus mirabilis*. *Microbiology* **2002**, *148*, 773−782.
(26) Stewart, P. S. Theoretical aspects of antibiotic diffusion into microbial biofilms. *J. Antimicrob. Chemother*. **1996**, *40*, 2517−2522.
(27) Stewart, P. S. A review of experimental measurements of effective diffuse permeabilities and effective diffusion coefficients in biofilms. *Biotechnol. Bioeng*. **1998**, *59*, 261−272.
(28) Mah, T.-F. C.; O'Toole, G. A. Mechanisms of biofilm resistance to antimicrobial agents. *Trends Microbiol*. **2001**, *9*, 34−38.
(29) Stewart, P. S.; Costerton, J. W. Antibiotic resistance of bacteria biofilms. *Lancet* **2001**, *358*, 135−138.
(30) Chambers, S. T.; Kunin, C. M. Isolation of glycine betaine and praline betaine from human urine. Assesment of their role as osmoprotective agents for bacteria and the kidney. *J. Clin. Invest*. **1987**, *79*, 731−737.
(31) Chambers, S. T.; Lever, M. Betaines and urinary tract infection. *Nephron* **1996**, *74*, 1−10.
(32) Jansen, A. M.; Lockatell, C. V.; Johnson, D. E.; Mobley, H. L. T. Visualization of *Proteus mirabilis* morphotypes in the urinary tract: the elongated swarmer cell is rarely observed in ascending urinary tract infection. *Infect. Immun*. **2003**, *71*, 3607−3613.
(33) Allison, C.; Coleman, N.; Jones, P. L.; Hughes, C. Ability of *Proteus mirabilis* to invade urothelial cells is coupled to motility and swarming differentiation. *Infect. Immun.* **1992**, *60*, 4740−4746.
(34) Keirsse, J.; Lahaye, E.; Bouter, A.; Dupont, V.; Boussard-Plédel, C.; Bureau, B.; Adam, J. L.; Monbet, V.; Sire, O. Mapping bacterial surface population physiology in real-time: infrared spectroscopy of *Proteus mirabilis* swarm colonies. *Appl. Spectrosc*. **2006**, *60*, 584−591.

BM070115W